EVALUATION OF THE CAUSES OF ERROR IN THE MCD45 BURNED-AREA PRODUCT FOR THE SAVANNAS OF NORTHERN SOUTH AMERICA

EVALUACIÓN DE LAS CAUSAS DE ERROR EN EL PRODUCTO DE ÁREA QUEMADA MCD45 PARA LAS SABANAS DEL NORTE DE SURAMÉRICA

SEBASTIÁN PALOMINO-ÁNGEL

Environmental Engineer, Environmental Engineering Program, Faculty of Engineering, Universidad de Medellín, Medellín, Colombia, spalomino@udem.edu.co

JESÚS A. ANAYA-ACEVEDO

PhD, Professor, Environmental Engineering Program, Faculty of Engineering, Universidad de Medellín, Medellín, Colombia, janaya@udem.edu.co

Received for review January 30 th, 2012, accepted September 25th, 2012, final version October, 19 th, 2012

ABSTRACT: Forest fires contribute to deforestation and have been considered a significant source of CO_2 emissions. There are global maps that estimate the area affected by a fire using the reflectance variation of the surface. In this study, we evaluated the reliability and the causes of error of the MCD45 Burned Area Product, by applying the confusion matrix method to the Orinoco River Basin. This basin is located in the northern zone of South America, and consists mainly of savanna ecosystems. For the evaluation, we used as reference data five pairs of Landsat images, covering 165,000 km^2. The Burned Area Product estimated a burned area of 7,576.43 km^2, which is lower than the area of 12,100.16 km^2 found with Landsat images, leading to an overall underestimation. The causes of error are associated to the spatial resolution of the map, and to some structures of the algorithm that generates the map.

KEYWORDS: burned area, Orinoco, forest fires, MCD45

RESUMEN: Los incendios forestales son considerados una causa significativa de deforestación y emisiones de CO_2. Existen productos globales que estiman el área afectada por el fuego utilizando las variaciones de reflectividad en la superficie terrestre. En este estudio se evaluó la fiabilidad y las causas de error del producto de área quemada MCD45, usando el método de matrices de confusión, para la cuenca hidrográfica del río Orinoco. Esta cuenca se ubica en la zona norte de Sur América, y predominan allí los ecosistemas de sabana. Para la evaluación se utilizó como información de referencia cinco pares de imágenes Landsat cubriendo 165.000 km^2. El producto de área quemada estimó un área afectada de 7.576,43 km^2, inferior a los 12.100,16 km^2 hallados con las imágenes Landsat. Esto indica una subestimación general, donde las causas de error están asociadas a la resolución espacial del mapa y a estructuras del algoritmo que genera el mismo.

PALABRAS CLAVE: área quemada, Orinoco, incendios forestales; MCD45

1. INTRODUCTION

Detecting areas burnt by forest fires is of great importance, given that fires are among the factors affecting the dynamics of ecosystems and their carbon and nutrient cycles [1]. They generate a significant impact on soil structure and loss of biodiversity, as well as greenhouse gas emissions [1–3].

Savanna ecosystems exhibit a high occurrence of fires throughout the world [4,5] and they are important on net carbon fluxes because of the large areas they occupy [6]. When the biomass present in a savanna is burnt, it becomes a major source of CO2 emissions in the atmosphere [7]. The Orinoco River basin in Colombia and Venezuela is the most representative tropical savanna in northern South America [8] and it is of particular interest due to the occurrence of fires during drought periods [4].

In South and Central America, it has been reported that CO2 emissions from biomass burning are between 8 and 9 times higher than emissions generated from fossil fuel consumption [9]. Deforestation rates have been used as

parameters to estimate greenhouse gas emmissions in this region [10–12]; however, [13] found that despite the reduction of deforestation rates in primary forests of the Brazilian Amazon, the expansion of grassland areas probably increases emissions via the burning activity needed to maintain these areas. Thereby, the importance of an estimation of the burned area in the region is evident.

Since 2000, global burned area products have been developed by using satellite data, each with a different spatial and temporal resolution. The most representative are GBA2000 [14], GLOBSCAR [15], MCD45 [16], and L3JRC [17]. These products detect the area directly affected by burning through algorithms from the carbon signal generated after the fire [3]. Burned area products have become an efficient alternative regarding time issues, costs, and spatial coverage in comparison to field methods used to monitor areas affected by fires [3,18].

It is necessary to quantify the accuracy of these products to determine the magnitude of the error, its causes, and implications. Global validation of the products should be developed with a regional approach, given that their global scale and fire characteristics are highly variable for different places. Most of the errors can be introduced because of: characteristics of the algorithm design, physical characteristics of the terrain, weather conditions in the area, vegetation type, and the intensity of the fire [19,20]. These aspects make it difficult to design an algorithm applicable to all areas and types of ecosystems throughout the world [21].

Systematic methods are being developed to assess the accuracy of global burned area maps on the regional level. So far, the best protocol for the selection of the reference data has been prepared by [22]. Evaluating the accuracy of these satellite data products has become a high-priority research topic [21,23,24].

Few studies have been conducted to estimate the burned area in the northern part of South America. Among the most important are those developed by [4,20,25]. However, results vary widely from one study to another; representing a major difficulty for the overall estimation of the burned area. Validating existing global burned area products helps to improve estimations of the burned area in the region and allows for the acquisition of information in a broader timeframe and a wider area.

The main objective of this study was to validate the spatial and temporal accuracy of the MCD45 global burned area product, emphasizing the causes of error. This product has the best spatial resolution of products currently available, and it is the only one that keeps generating data. We performed the validation on the Orinoco River Basin in northern South America between Colombia and Venezuela using the confusion matrix method and reference data from Landsat Enhanced Thematic Mapper Plus, ETM+, images. Three factors considered to be causes of error were analyzed: the presence of clouds, the effect of pixel size, and the type of vegetation being burned.

2. MATERIALS AND METHODS

2.1. Study area

The validation of the MCD45 burned area product was held in the ecoregion known as *Los Llanos* with an area of 375,081 km^2 in the Orinoco River basin. This basin consists of more than 1,000,000 km^2 of land, characterized by heterogeneous savanna ecosystems, which vary according to factors such as soil, flooding, and vegetation types [4]. The proportion of vegetation according to the MCD12Q1 global vegetation map is: grassland (30%), savanna woodlands (27%), savannas (16%), a mosaic of natural vegetation and crops (14%), and evergreen broadleaf forest (13%).

The area has a temperature ranging from 23 to 30 °C, depending on the time of year [25]; the lowest temperatures are recorded during the rainy season and the higher temperatures in the drier months. Rainfall in the area ranges between 1500 and 3500 mm, as an annual average [26]. The basin presents monomodal behavior, with a marked rainy season that runs from April to November and a dry season between December and March [26,27].

The main economic activities in the area are agriculture (palm oil and rice), with extensive livestock activity, mining, oil exploration and extraction, silviculture, and ecotourism [4,26]; extensive livestock being the most important [4] economic activity. These anthropogenic activities are the major cause of forest fires in the area [4,28].

2.2. Reference data

Reference information gathered in the field and free of errors is required to validate the MCD45 burned

area product; however, it is difficult and expensive to collect such information in the field, mainly because of the restricted access to the affected area, the ephemeral nature of the signal, and the great extension of the fires. However, satellite images of higher spatial resolution than the product being validated is an alternative method to data collection in the field [22]. In this case, a product of 500 m pixel size was validated with 30 m satellite images [20,25,29].

In this study, Landsat Enhanced Thematic Mapper Plus (ETM+) images were used as reference data, [30] has shown the applicability of Landsat images in Colombia to produce vegetation maps. Each Landsat image covers approximately 34,225 km^2, and has a 30 m spatial resolution [31]. Five pairs of images were used in the study, each corresponding to a different location, according to the unique Landsat reference system: Worldwide Reference System (WRS). This reference system assigns a Path/Row location for each image around the world. Each pair of images has the same geographical area, and about a month of difference in time between the images that compose the pair. This method allows for one to establish the time period where a fire has occurred. It also helps to avoid errors in the reference data due to confusion with dark soils, water bodies, and cloud shadows, which have similar reflectivity characteristics to the burned areas [22].

Images were selected for the dry season and with the lowest possible cloud content. The total area assessed was approximately 165,000 km^2, which corresponds to 16.5% of the total basin area.

After reviewing the available pairs of images, only those images which met the previously-described criteria were selected, ensuring reliable reference information for validation. Table 1 lists the selected Landsat images (with their corresponding date) used to obtain reference information.

Table 1. Pairs of Landsat images selected as reference

Landsat (Path/Row)	Date (Year/Month/Day)
004/054	2002/12/30 and 2003/01/31
005/055	2002/01/03 and 2002/02/20
005/056	2003/01/06 and 2003/01/22
005/057	2003/01/06 and 2003/01/22
006/055	2001/01/23 and 2001/02/24

2.3. Global burned area product

The MCD45 burned area product is generated from multi-temporal observations of the earth's surface reflectivity for a determined period of time. An algorithm is generated based on the bi-

directional reflectance model-based change detection developed by [3] and improved by [16] to continuously map fire-affected areas. The algorithm uses the reflectance sensed within a period of time of a fixed number of days to predict the reflectance on a subsequent day. It is determined whether the difference between the predicted and observed reflectance is relevant [3]. After that, some tests are applied to each pixel to determine which would be a candidate for burning [3,16].

When a pixel becomes a candidate for burning but does not pass all the tests because of insufficient observations, an iterative search method is used prior to discarding it. This method is based on the fact that there is a high probability finding burned pixels neighboring confidently-detected burns [3,16]. In subsequent sections, we will refer to this method as *context algorithm*.

The MCD45 product provides information about the date of the detection of the burnt area. This data indicates the presence of a burn signal and the approximate date of burning. The product also provides information about the quality of the detection made, the presence of snow, water bodies, and areas where there were insufficient data to do detection work [1].

The MCD45 product has a global coverage and 500 m spatial resolution. It has been available from the year 2000 onwards, and is generated in one-month time periods, including an 8-day presicion before and after each day [1].

2.4. Data processing

2.4.1. Reference data

The reference data was obtained from the visual interpretation of the 5 pairs of orthorectified Landsat images ETM+. An RGB false color with bands 3 (0.63 to 0.69 μm), 4 (0.76 to 0.90 μm), and 5 (1.55 to 1.75 μm) was used to improve the visual identification of burned

areas. Figure 1 shows the delimitation process of the reference burned area found in the Landsat images. Only those burned areas occurring after the first acquisition date are polygon digitized. From these polygons, a raster dichotomic map was generated (with only two pixel values: burned and unburned) with a 30 m spatial resolution, according to the reference-image pixel size.

2.4.2. Global burned area product

The MCD45 is provided with sinusoidal projection and was reprojected to the UTM Zone 19N WGS84. The product was processed to generate a raster dichotomic map with a 500 m spatial resolution, but including only those pixels identified between the Landsat acquisition dates (Fig. 1). The new map was re-sampled reducing pixel size to 30 m; therby, the results obtained could be compared to those generated by the high-resolution Landsat images.

2.5. Validation

The confusion matrix was used to evaluate the spatial accuracy of the MCD45 product. This method consists of building a square matrix, where columns contain the reference data and rows contain the information of the product being validated. Thus, the major diagonal of the matrix only has those pixels correctly classified [32]. The matrix allows for one to identify two types of errors: omission errors, which correspond to areas that were really burned and were not classified as such in the MCD45 product; and commission errors, related to areas classified as "burnt" in the product but that were not really burnt. The matrix also allows for one to calculate two indices: the overall accuracy, which offers an estimate of the total percentage of product success; and the Kappa coefficient, which indicates whether the agreement between the classification made by the MCD45 product and the reference data is significant. To determine this relationship, [32], based on the definition of [33], proposed classifying the Kappa coefficient value in the following ranges: less than 0.00 there is no agreement; between 0.00 and 0.20 there is poor agreement; between 0.21 and 0.40 there is slight agreement; between 0.41 and 0.60 there is moderate agreement; between 0.61 and 0.80 ther is substantial agreement; and between 0.81 and 1.00 there is strong agreement among the information.

2.6. Identification of causes of error

According to previous studies, the sources of error can be associated with spatial and temporal

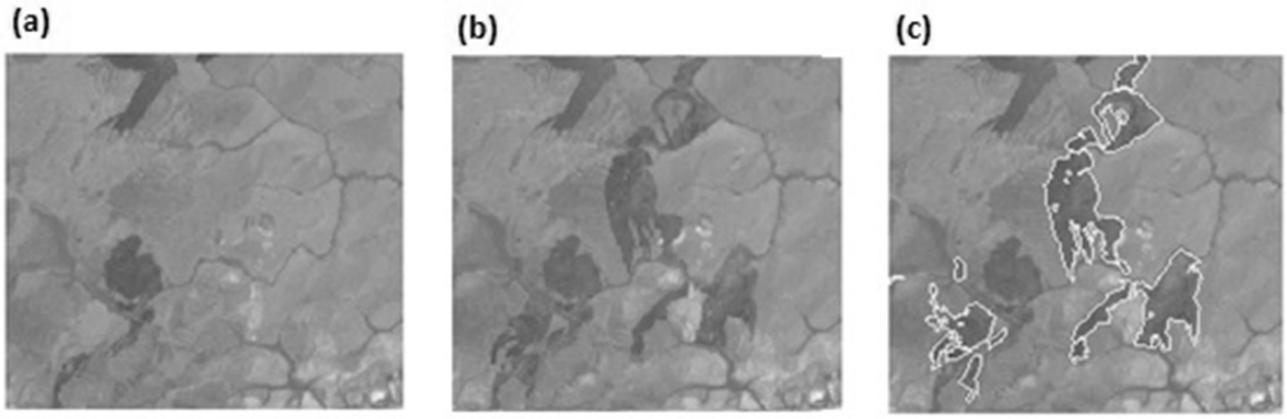

Figure 1. Delimitation of burned area by using a subset of Landsat image 005/056: (a) shows the first acquisition Landsat image of the pair (2003/01/06), (b) shows the second acquisition Landsat image of the pair (2003/01/22) where the burned area can be visually identified, (c) shows the burned area identified between acquisitions

resolution, the presence of clouds (weather conditions) or smoke plumes, confusion with dark surfaces, vegetation type in the study area (physical characteristics of the terrain) and weaknesses in the algorithm [19–21,29]. Because the study area was a tropical zone, the analysis of the presence of clouds was emphasized by using a cloud mask for the period evaluated in each pair of reference images. We also analyzed the effect of the 500 m pixel in the errors of omission and commission (spatial resolution effect) and the vegetation type in the study area.

2.6.1. Spatial resolution

Errors caused by discritizing a surface into pixels resulted in two types of error: omission, when the burned areas are smaller than the pixel size; and commission, when mixed pixels include both burned pixels and unburned pixels.

Omission errors: The incidence of spatial resolution in the omission errors was assessed by identifying the burned reference polygons with an area smaller than the pixel size of the MCD45 product; i.e., 0.22 km2. It is expected that the product does not identify an area smaller than the size of its pixel as a burned area.

A new reference map was generated containing only these areas and it was overlaid with MCD45 to determine the proportion of polygons with area > 0.22 km2, not identified by MCD45. This error was quantified in terms of the proportion of total area omitted.

Commission errors: Regarding the errors of commission, it was found that the MCD45 product includes unburned areas outside polygons identified as burnt, mainly in their border regions. This is due to the pixel size of the product and to the context algorithms (when used), increasing the probability of commission along the borders of burned areas. Because of this, in order to evaluate the impact of these factors on commission errors, a 500 m corridor (according to the spatial resolution of the MCD45 product) was built around each of the polygons of the reference map, to identify what percentage of the total commission error is located within this corridor.

2.6.2. Cloud cover

The influence of cloud presence over the study area was evaluated as omission. For this analysis, a cloud mask was used to cover the period of the exact dates of the pairs of images used as reference. We determined the portion of the total reference area and the total omission error that presented cloudiness during the evaluated time period. Aditionally, the influence of cloud shadow on the commission error was visually evaluated.

2.6.3. Vegetation type

According to the MCD12Q1 global vegetation map, most representative cover in the study area is grassland, savanna woodlands, savannas, a mosaic of natural vegetation and crops, and evergreen broadleaf forest. We determined here the proportion of the omission and commission error area over each vegetation type, by overlaping the information about the errors obtained previously with the MCD12Q1 global vegetation map in the study area.

3. RESULTS

3.1. Validation

The 5 pairs of Landsat images used cover an area of 171,125 km2. As mentioned above, the zones of the images where a precise identification of the burned area of reference could not be guaranteed were not considered for validation. That is why the total assessed area was 165,000 km2.

Figure 2 presents the area detected as burned by the MCD45 product during the January 2003 period. This result was validated with information from the pairs of Landsat images taken for the same dates, corresponding to the Landsat *Path/Row*: 004/054, 005/056, and 005/057. Figure 2 shows the geographical extent of the validation area. A similar map was generated for January and February 2001 and for January and February 2002, used to evaluate the Landsat *Path/Row*: 006/055 and 005/055, respectively.

The validation for each Landsat pair is presented in Tables 2 and 3, respectively. A total of 18,447 reference polygons were delimited, in comparison with the 4,224 polygons estimated by the MCD45 product. We found a minimum area of 0.001 km2 and a maximum of 169 km2 for the reference polygons, with an average polygon size of 0.66 km2. For the MCD45 product, we found that the smallest polygon area covers 0.22 km2 and the largest is of 142.1 km2, with an average polygon size of 1.83 km2. The difference in the minimum area of polygons is due to the spatial resolution of each map.

We also found that digitized polygons represent 7.1% (12,100.16 km2) of the total area evaluated. On the other hand, the MCD45 product estimated a total

burned area of 7,576.43 km2, which represents 4.4% of the total area assessed.

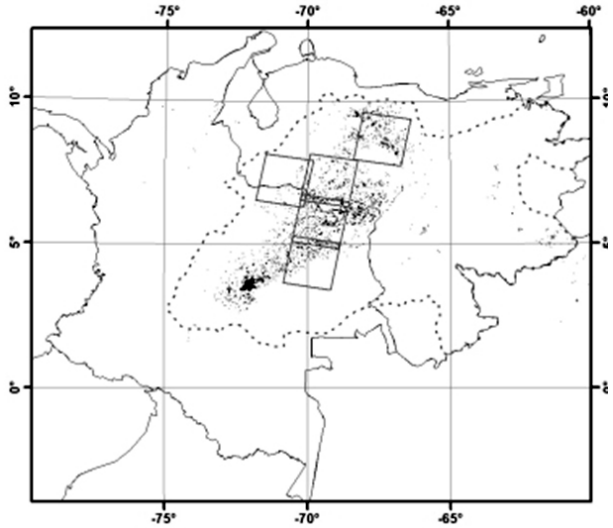

Figure 2. Burned area identified by the MCD45 product for January 2003. Black shows the areas classified as burnt, the squares represent the limits of the five validation areas, and the dotted line indicates the limits of the Orinoco basin.

Table 2. Number of polygons identified as burnt and total burnt area in each zone of study, according to the 5 pairs of Landsat images used as reference

Landsat path/row	Number of polygons	Burnt area (km^2)	% burnt in the image
004/054	3,733	2,891.56	8.4
005/055	7,914	4,148.10	12.2
005/056	1,937	2,168.96	6.3
005/057	2,982	1,958.39	5.7
006/055	1,881	933.15	2.7

Table 3. Number of polygons identified as burnt and total burnt area in each zone of study, according to the classification of the MCD45 product

Landsat path/row	Number of polygons	Burnt area (km^2)	% burnt in the image
004/054	1,147	2,263.06	6.6
005/055	861	1,215.91	3.6
005/056	973	2,125.71	6.2
005/057	971	1,561.18	4.5
006/055	292	410.57	1.2

Underestimation of the burned area via MCD45 is observed for all areas of study. This underestimation is due to the fact that errors of omission are higher than errors of commission. It is important to note that one should not consider that the commission partially compensates the omission. It would not be correct to state that an omission of an ecosystem (for instance, a forest) is compensated by a commission in another different ecosystem (for example a grassland), as the biomass affected is different in each of them.

The results of the errors and coefficients obtained from the confusion matrix by comparing the reference information with the information from the MCD45 product are presented in Table 4.

The overall accuracy of the classification (column 2, Table 4) refers to the percentage of pixels correctly classified by MCD45 (taking into account pixels classified as burnt and unburnt) compared with the total number of pixels of reference. We obtained very high values in this measure, with the lowest at 88.80% and the highest at 96.74%. This is mainly because more than 90% of the agreements were from the unburned class, and therefore, this measure is not representative of the level of agreement that exists in the identification of the burned area. The commission and omission errors of a burned area were also caculated (Table 4, respectively) to illustrate in detail the performance of the MCD45 product. We observed that commission errors are significantly lower than the omission errors, except for the 005/056 image, where a similar value for the two errors was presented. Therefore, a general underestimation of the burned area in the study zone is observed. The product's developers have generally concentrated greater efforts on reducing commission errors, perhaps because it is not convenient for a user to invest resources in visiting an area identified as burnt for the product, when it really is not [29].

According to the Kappa coefficient analysis, there is a substantial agreement for one of the evaluated images (005/056), a moderate agreement for two images (004/054 and 005/057), and slight agreement for the two remaining images (005/055 and006/055) of the

study. From a mean calculation of the Kappa values for the different images, we determined that there is moderate agreement for the total area of reference. However, it is important to note that there is a high variability of coefficient values, as well as of omission errors among the images used. Previous studies such as [33,34] established that such a variation may be caused by several factors including the type of fire and the vegetation burned.

Table 4. Results of the confusion matrix

Landsat path/row	Overall Accuracy (%)	Comm. Error (%)	Omiss. Error (%)	Kappa Coeff.
004/054	93.53	34.63	50.39	0.53
005/055	88.80	36.32	81.35	0.25
005/056	95.92	31.69	33.15	0.65
005/057	96.02	31.08	45.06	0.59
006/055	96.74	47.57	76.91	0.31

3.2. Causes of error

3.2.1. Spatial resolution

An analysis of polygons with areas smaller than the MCD45 pixel size (0.22 km2) was performed, to evaluate the effect of the spatial resolution on the omission error (Table 5).

We found that 97.2% of the polygons with an area < 0.22 km2 are omitted for the study area. Through visual evaluation, we found that the 2.8% of the polygons with an area < 0.22 km2 identified as burned correspond to the polygons near the borders of larger burned areas which, due to the size of the pixel of the MCD45, were also classified as burned.

The polygons omitted, with an area < 0.22 km2, represent 6.3% of the total burned area of reference, suggesting that part of the total omission error is generated due to the minimum mapping unit that MCD45 is able to identify.

We also assessed the influence of spatial resolution and context algorithms on the commission error and found that, on average, 81.3% of the commission errors are within the 500 m corridors outside the reference polygons (Table 6). The 006/055 image presented the minimum value, and had 71.1% of the commission located within the corridors. Image 005/055 presented the maximum value and had 96.0% of the commission located within the corridors.

Table 5. Influence of the spatial resolution on the total omission error for burned polygons with an area smaller than 0.22 km^2

Landsat path/ row	Total area contained in polygons with < 0.22 km^2 (km^2)	Area identified by MCD45 (km^2)	Area omitted by MCD45 (km^2)
004/054	170.89	6.76	164.13
005/055	310.20	7.46	302.74
005/056	79.62	2.69	76.93
005/057	135.67	2.94	132.73
006/055	84.65	2.36	82.29

Additionally, via visual evaluation, we found that the remaining commission is mostly located in burned areas that were not identified by the product at the time of its occurrence, but in subsequent periods. This is not an error regarding the spatial distribution of a burned area; however, it represents an error in relation to the temporal accuracy of the product.

3.2.2. Cloud cover

Based on the cloud mask used, we found that 17,000 km^2 (10.3% of the study area) showed clouds during the evaluated period. This means that it was possible for the MCD45 to make a correct observation of the surface for the remaining area during the study.

The burned area omitted by MCD45 was 7,149.08 km^2. Only 687.79 km^2 of this area (9.6%) showed cloudiness during the evaluated period. This suggests that more than 90.0% of the omitted area was located in zones free of clouds.

During a visual evaluation, we found that none of the

commission errors were associated with shadows from the clouds.

Table 6. Influence of the spatial resolution on the total commission area (CA)

Landsat path/row	Total CA (km^2)	CA located outside the corridors (km^2)	CA located within the corridors (km^2)
004/054	759.77	193.89	565.88
005/055	441.14	17.46	423.68
005/056	672.56	136.92	535.64
005/057	485.16	72.50	412.66
006/055	195.50	56.50	139.00

3.2.3. Vegetation type

We found that the burned area is mostly located in grassland, savanna woodland, and savanna covers; the grassland being the most affected vegetation type. The mosaic of natural vegetation and crop cover, and evergreen broadleaf forest cover present less burned area (Table 7).

In the proportion of error by vegetation type analysis, we found that there is more commission than omission for the grassland cover, and there is more omission than commission for the savanna woodlands cover (Table 7).

4. CONCLUSION

The MCD45 map underestimates the burned area in the study zone by 37.4%. This is mainly due to the existence of both omission and commission errors, but one does not compensate for the other in terms of area; and the first greatly exceeds the latter. The implications of this situation on certain applications should be addressed specifically. The results are consistent with the findings reported by [29] in South Africa.

Most of the commission errors (81.3%) in the study area are related to the spatial resolution of the product and the context algorithms; however, these algorithms also contribute to reducing the omission. Much of the remaining commission

Table 7. Proportion of total burned area based on vegetation type and type of error

Vegetation type	Total burned area (%)	Omission error (%)	Commission error (%)
Grassland	48.0	41.0	50.0
Savanna woodland	28.0	32.9	25.0
Savannas	19.0	19.7	19.8
Mosaic of natural vegetation and crops	4.2	5.2	4.5
Evergreen broadleaf forest	0.8	1.2	0.7
Total	100	100	100

error was found in areas burned from previous periods, but which were not identified at the time of their occurrence; this is why they do not represent a commission error, given that the spatial distribution of the burned area is not affected. It does represent an error in the product's temporal precision. None of the commission errors were associated with cloud shadows. Omission errors represent a difficulty for the MCD45 at the moment of the total burned area estimation. Some 52.8% of the burned area was omitted for reasons beyond the map spatial resolution. Additionally, it was found that despite the existence of selected zones and dates significantly free of cloudiness, the omission of the burned area remains a problem, indicating the precence of other factors like soil moisture, type of fire, and vegetation burned [34,35], influencing the omission and requiring a further detailed study.

Fires in the study area seem to be more related to grassland, savanna woodland, and savanna-cover type in the study area. The distribution of the omission error shows more influence over savanna woodland, and the commission error over the grassland covers. Further evaluations should be conducted in other regions and time periods to complement those observations about

the vegetation-type influence over the omission and commission errors.

ACKNOWLEDGEMENTS

This work was supported by *Universidad de Medellín* and *Colciencias* through the Program *Jóvenes investigadores e innovadores, Virginia Gutiérrez de Pineda.*

REFERENCES

[1] Boschetti, L., Roy, D. P. and Hoffmann, A., MODIS Collection 5 Burned Area Product - MCD45 User's guide, University of Maryland, South Dakota State University, LM University of Munich, 2009.

[2] Watson, R. T., Noble, I. R., Bolin, B., Ravindranath, N. H., Verardo, D. J. and Dokken, D. J., Special Report on Land Use, Land Use Change and Forestry, Cambridge University Press, Cambridge, 2000.

[3] Roy, D. P., Lewis, P. E. and Justice, C. O., Burned area mapping using multi-temporal moderate spatial resolution data a bi-directional reflectance model-based expectation approach, Remote Sensing of Environment, 83, pp. 263–286, 2002.

[4] Romero, M., Etter, A., Sarmiento, A. and Tansey, K., Spatial and temporal variability of fires in relation to ecosystems, land tenure and rainfall in savannas of northern South America, Global Change Biology, 16, pp. 2013 – 2023, 2009.

[5] Hao, W. M. and Liu, M. H., Spatial and temporal distribution of tropical biomass burning, Global Biogeochemical Cycles, 8, pp. 495–503, 1994.

[6] San José, J. J. and Montes, R. A., Management effects on carbon stocks and fluxes across the Orinoco savannas, Forest ecology and management, 150, pp. 293 – 311, 2001.

[7] Mouillot, F., Narasimha, A., Balkanski, Y., Lamarque, J. F. and Field, C. B., Global carbon emissions from biomass burning in the 20th century, Geophysical Research Letters, 33, L01801, 4, 2006.

[8] Berrio, J. C., Hooghiemstra, H., Behling, H., Botero, P. and Van Der Borg, K., Late-Quaternary savanna history of the Colombian Llanos Orientales from Lagunas Chenevo and Mozambique: a transect synthesis, The Holocene, 12, pp. 35-48, 2002.

[9] Liousse, C., Andreae, M. O., Artaxo, P., Barbose, P., Cachier, H., Grégoire, J. M., Hobbs, P., Lavoué, D., Mouillot, F., Penner, J., Scholes, M. and Schultz, M., Deriving Global Quantitative Estimates for Spatial and Temporal Distributions of Biomass Burning Emissions, In: Emissions of atmospheric trace compounds (Eds. P. Artaxo and C. E. Reeves), Kluwer Academic Publishers, 2004.

[10] Naughton, L., Deforestation and Carbon Emissions at Tropical Frontiers: A Case Study from the Peruvian Amazon, World Development, 32, pp. 173-190, 2004.

[11] Defries, R., Achard, F., Brown, S., Herold, M., Murdiyarso, D., Schlamadinger, B. and De Souza JR, C., Earth observations for estimating greenhouse gas emissions from deforestation in developing countries, Environmental Science and Policy, 10, pp. 385-394, 2007.

[12] Fearnside, P. M., Righi, C. A., Lima De Alencastro, P. M., Keizer, E. W., Cerri, C. C., Melo, E. and Imbrozio, R., Biomass and greenhouse-gas emissions from land-use change in Brazil's Amazonian ''arc of deforestation'': The states of Mato Grosso and Rondonia, Forest Ecology and Management., 258, pp. 1968-1978, 2009.

[13] Guild, L. S., Kauffman, J. B., Cohen, W. B., Hlavka, C. A. and Ward, D., Modeling Biomass Burning Emissions Amazon Forest and Pastures in Rondonia, Brazil, Ecological Society of America, 14, pp. s232-s246, 2004.

[14] Grégoire, J.-M., Tansey, K. and Silva, J. M. N., The GBA2000 initiative: developing a global burnt area database from SPOT-VEGETATION imagery, International Journal of Remote Sensing, 24, pp. 1369-1376, 2003.

[15] Simon, M., Plummer, S., Fierens, F., Hoelzemann, J. J. and Arino, O., Burnt area detection at global scale using ATSR-2: The GLOBSCAR products and their qualification, Journal of Geophysical Research, 109, D14S02, 2004.

[16] Roy, D. P., Jin, Y., Lewis, P.E. and Justice, C. O., Prototyping a global algorithm for systematic fire-affected area mapping using MODIS time series data, Remote Sensing of Environment, 97, pp. 137–162, 2005.

[17] Tansey, K., Grégoire, J. M., Pereira, J. M. C., Defourny, P., Leigh, R., Pekel, J. F., Barros, A., Silva, J., Van Bogaert, E., Bartholomé, E. and Bontemps, S., L3JRC - A global, multi - year (2000 - 2007) burnt area product (1 km resolution and daily time steps). Remote Sensing and Photogrammetry Society Annual Conference 2007. Newcastle upon Tyne, UK, 11-14, September 2007.

[18] Bella, C. M. D., Jobbágy, E. G., Paruelo, J. M. and Pinnock, S., Continental fire density patterns in South America, Global Ecology and Biogeography, 15, pp. 192-199, 2006.

[19] Roy, D. P. and Landmann, T., Characterizing the surface heterogeneity of fire effects using multi-temporal reflective wavelength data, International Journal of Remote Sensing, 20, pp. 4197-4218, 2005.

[20] Anaya, J. A. and Chuvieco, E., Validación para Colombia de la estimación de área quemada del Producto L3JRC en el periodo 2001-2007, Actualidades Biológicas, 32, pp. 29-40, 2010.

[21] Opazo, S. and Chuvieco, E., Cartografía de áreas quemadas en Sudamérica: Detección de píxeles semilla, Revista de Teledetección, 32, pp. 50-71, 2009.

[22] Boschetti, L. and Roy, D.P., International Global Burned Area Satellite Product Validation Protocol Part I – production and standardization of validation reference data. Unpublished data.

[23] Foody, G. M., Status of land cover classification accuracy assessment, Remote Sensing of Environment, 80, pp. 185-201, 2002.

[24] Boschetti, L., Flasse, S. P. and Brivio, P. A., Analysis of the conflict between omission and commission in low spatial resolution dichotomic thematic products: The Pareto Boundary, Remote Sensing of Environment, 91, pp. 280–292, 2004.

[25] Armenteras, D., Romero, M. and Galindo, G., Vegetation fire in the savannas of The Llanos Orientales of Colombia, World Resource Review, 17, pp. 628 – 638, 2005.

[26] Correa, H. D., Ruiz, S. L. and Arévalo, L. M., Plan de acción en biodiversidad de la cuenca del Orinoco – Colombia / 2005 - 2015 – Propuesta Técnica. Bogotá D.C.: Corporinoquia, Cormacarena, I.A.v.H, Unitrópico, Fundación Omacha, Fundación Horizonte Verde, Universidad Javeriana, Unillanos, WWF - Colombia, GTZ – Colombia, 2005.

[27] Etter, A., Cháves, M.E. and Arango, N., Informe nacional sobre el estado de la biodiversidad-Colombia 1997. Bogotá D.C.: Instituto Humboldt, PNUMA, Ministerio del Medio Ambiente, Colombia, 1998.

[28] MAVDT. Plan nacional de prevención, control de incendios forestales y restauración de áreas afectadas. Bogotá D.C.: Ministerio de Ambiente Vivienda y Desarrollo Territorial de Colombia, 2002.

[29] Roy, D. P. and Boschetti, L., Southern Africa Validation of the MODIS, L3JRC and GlobCarbon Burned-Area Products, IEEE Transactions on Geoscience and Remote Sensing, 47, pp. 1032 – 1044, 2009.

[30] Polanco, J. A., Teledetección de la vegetación del Páramo de Belmira con imágenes Landsat, Dyna, 171, pp. 222-231, 2012.

[31] NASA. Landsat 7 Science Data Users Handbook. Maryland: National Aeronautics and Space Administration, 2009.

[32] Congalton, R. G. and Green, K., Assessing the Accuracy of Remotely Sensed Data: Principles and Practices, 2nd ed., CRC Press Taylor & Francis Group, 2009.

[33] Landis, J. R. and Koch, G. G., The Measurement of Observer Agreement for Categorical Data, Biometrics, 33, pp. 159 – 174, 1977.

[34] Pereira, J. M. C., Mota, B., Privette, J. L., Caylor, K. K., Silva, J. M. N., Sa, A. C. L. and Ni-Meister, W., A simulation analysis of the detectability of understory burns in miombo woodlands, Remote Sensing of Environment, 93, 296–310, 2004.

[35] Silva, J.M.N., Sa, A. C. L. and Pereira, J. M. C., Comparison of burned area estimates derived from SPOT-VEGETATION and Landsat ETM+ data in Africa: Influence of spatial pattern and vegetation type, Remote Sensing of Environment, 96, pp. 188–201, 2005.